TEAM: ThrEshold Adaptive Memristor Model

Shahar Kvatinsky, Eby G. Friedman, *Fellow, IEEE*, Avinoam Kolodny, *Senior Member, IEEE*, and
Uri C. Weiser, *Fellow, IEEE*

Abstract—**Memristive devices are novel devices, which can be
used in applications ranging from memory and logic to neuro-
morphic systems. A memristive device offers several advantages:
nonvolatility, good scalability, effectively no leakage current, and
compatibility with CMOS technology, both electrically and in
terms of manufacturing. Several models for memristive devices
have been developed and are discussed in this paper. Digital ap-
plications such as memory and logic require a model that is highly
nonlinear, simple for calculations, and sufficiently accurate. In
this paper, a new memristive device model is presented—TEAM,
ThrEshold Adaptive Memristor model. This model is flexible and
can be fit to any practical memristive device. Previously published
models are compared in this paper to the proposed TEAM model.
It is shown that the proposed model is reasonably accurate and
computationally efficient, and is more appropriate for circuit
simulation than previously published models.**

Index Terms—**Memristive systems, memristor, SPICE, window
function.**

I. INTRODUCTION

MEMRISTORS are passive two-port elements with
variable resistance (also known as a memristance) [1].
Changes in the memristance depend upon the history of the
device (e.g., the memristance may depend on the total charge
passed through the device, or alternatively, on the integral over
time of the applied voltage between the ports of the device).

Formally, a current-controlled time-invariant memristive
system [2] is represented by

$$\frac{dw}{dt} = f(w, i), \qquad (1)$$

$$v(t) = R(w, i) \cdot i(t), \qquad (2)$$

where w is an internal state variable, $i(t)$ is the memristive de-
vice current, $v(t)$ is the memristive device voltage, $R(w, i)$ is
the memristance, and t is time. The terms memristor and mem-
ristive systems are often used interchangeably to describe mem-
ristive systems [2]. While there are discussions in the literature
about specific definitions [29], [30], in this paper we use the
term "memristive device" to describe all devices within these
categories.

Since Hewlett-Packard announced the fabrication of a
working memristive device in 2008 [3], there has been an

increasing interest in memristors and memristive systems. New
devices exhibiting memristive behavior have been announced
[4], [5], and existing devices such as spin-transfer torque mag-
netoresistive random access memory (STT-MRAM) have been
redescribed in terms of memristive systems [6].

Memristive devices can be used for a variety of applications
such as memory [7], neuromorphic systems [8], analog circuits
(e.g., see [9]), and logic design [10], [27]. Different characteris-
tics are important for the effective use of memristive devices in
each of these applications, and an appropriate designer friendly
physical model of a memristive device is therefore required.

In this paper, the characteristics of memristive devices are
described in Section II. Previously published memristive de-
vice models are reviewed in Section III. TEAM—a new model
that is preferable in terms of the aforementioned characteris-
tics—is proposed in Section IV. In Section V, a comparison be-
tween these models is presented. The paper is summarized in
Section VI.

II. REQUIREMENTS FOR MEMRISTIVE DEVICE CHARACTERISTICS

Different applications require different characteristics from
the building blocks. Logic and memory applications, for ex-
ample, require elements for computation and control, as well
as the ability to store data after computation. These elements re-
quire sufficiently fast read and write times. The read mechanism
needs to be nondestructive, i.e., the reading mechanism should
not change the stored data while reading. To store a known dig-
ital state and maintain low sensitivity to variations in parame-
ters and operating conditions, it is crucial that the stored data be
distinct, i.e., the difference between different data must be suf-
ficiently large. The transient power consumption while reading
and writing, as well as static power consumption, are also crit-
ical issues.

Although the definition of a memristive system is quite broad,
all memristive systems exhibit a variable resistance, which is re-
lated to an internal state variable. Memristive devices employed
in practice exhibit a nonvolatile behavior. To provide a non-
destructive read mechanism, the internal state variable needs
to exhibit a nonlinear dependence on charge, i.e., changes in
the state variable due to high currents should be significant,
while changes due to low currents should be negligible. Other
mechanisms where the state variables return to the original po-
sition after completing the read process may also require the
nondestructive read mechanism. For certain applications such
as analog counters, however, a linear dependence on charge is
preferable, since the current is integrated during the counting
process.

To store distinct Boolean data in a memristive device, a high
ratio between the resistances (typically named R_{ON} and R_{OFF})
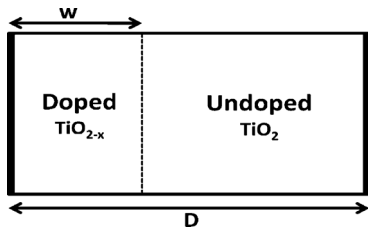is necessary. Several additional characteristics are important for

Fig. 1. Linear ion drift memristive device model. The device is composed of two regions: doped and undoped. The total resistance of the device is the sum of the resistance of both regions.

all applications, such as low power consumption, good scalability, and compatibility with conventional CMOS.

These characteristics exist in memristive devices. STT-MRAM exhibits these characteristics except for the high off/on resistance ratio [11]. To design and analyze memristive device-based circuits and applications, a model exhibiting these traits is required.

III. PREVIOUSLY PROPOSED MEMRISTIVE DEVICE MODELS

A. Requirements From an Effective Memristive Device Model

An effective memristive device model needs to satisfy several requirements: it must be sufficiently accurate and computationally efficient. It is desirable for the model to be simple, intuitive, and closed-form. It is also preferable for the model to be general so that it can be tuned to suit different types of memristive devices.

B. Linear Ion Drift Model

A linear ion drift model for a memristive device is suggested in [3]. In this model, one assumption is that a device of physical width D contains two regions, as shown in Fig. 1. One region of width w (which acts as the state variable of the system) has a high concentration of dopants (originally oxygen vacancies of TiO_2, namely TiO_{2-x}). The second region of width $D - w$ is an oxide region (originally TiO_2). The region with the dopants has a higher conductance than the oxide region, and the device is modeled as two resistors connected in series. Several assumptions are made: ohmic conductance, linear ion drift in a uniform field, and the ions have equal average ion mobility μ_V. Equations (1) and (2) become, respectively,

$$\frac{dw}{dt} = \mu_v \frac{R_{ON}}{D} i(t), \tag{3}$$

$$v(t) = \left(R_{ON} \frac{w(t)}{D} + R_{OFF} \left(1 - \frac{w(t)}{D} \right) \right) \cdot i(t), \tag{4}$$

where R_{ON} is the resistance when $w(t) = D$, and R_{OFF} is the resistance when $w(t) = 0$. The state variable $w(t)$ is limited to the physical dimensions of the device, i.e., the value is within the interval $[0, D]$. To prevent w from growing beyond the physical device size, the derivative of w is multiplied by a window function, as discussed in Section III-C. The I-V curve of a linear ion drift memristive device for sinusoidal and rectangular waveform inputs is shown in Fig. 2.

C. Window Function

In the linear ion drift model, the permissible value of the state variable is limited to the interval $[0, D]$. To satisfy these bounds, (3) is multiplied by a function that nullifies the derivative, and
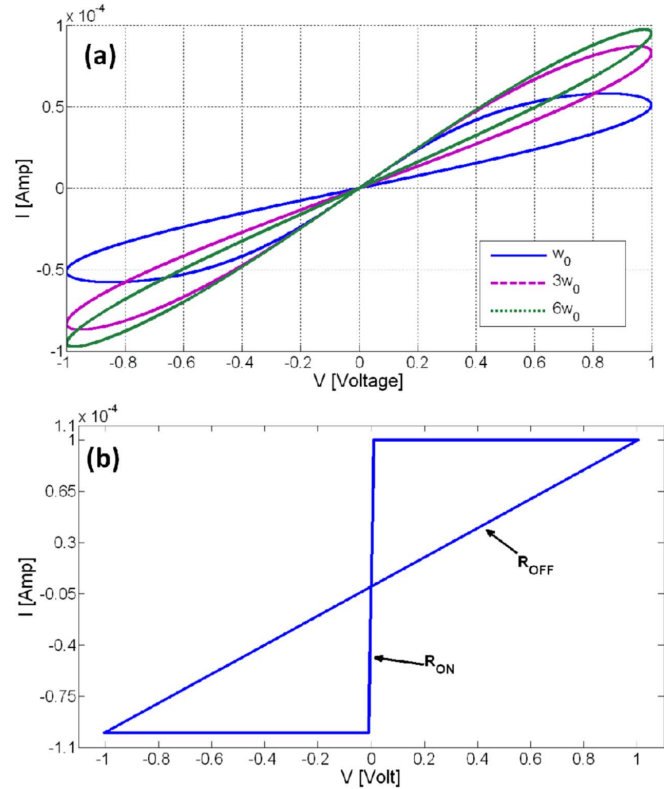

Fig. 2. Linear ion drift model I-V curve. $D = 10$ nm, $R_{ON} = 100 \ \Omega$, $R_{OFF} = 16$ kΩ, $\mu_V = 10^{-14}$ m^{2}s^{-1}V^{-1}, and $w_0 = 1$ Rad/s. (a) Sinusoidal voltage input for several frequencies ω_0, $3\omega_0$, and $6\omega_0$, and (b) rectangular waveform current input.

forces (3) to be identical to zero when w is at a bound. One possible approach is an ideal rectangular window function (the function where the value is 1 for any value of the state variable, except at the boundaries where the value is 0). It is also possible to add a nonlinear ion drift phenomenon, such as a decrease in the ion drift speed close to the bounds, with a different window [12],

$$f(w) = 1 - \left(\frac{2w}{D} - 1 \right)^{2p}, \tag{5}$$

where p is a positive integer. For large values of p, the window function becomes similar to a rectangular window function, and the nonlinear ion drift phenomenon decreases, as shown in Fig. 3.

The window function in (5) exhibits a significant problem for modeling practical devices, since the derivative of w is forced to zero and the internal state of the device cannot change if w reaches one of the bounds. To prevent this modeling inaccuracy, a different window function has been proposed [13],

$$f(w) = 1 - \left(\frac{w}{D} - stp(-i) \right)^{2p}, \tag{6}$$

$$stp(i) = \begin{cases} 1, & i \geq 0 \\ 0, & i < 0, \end{cases} \tag{7a} \tag{7b}$$

where i is the memristive device current. This function is shown in Fig. 4. In the original definition, these window functions do not have a scale factor and therefore cannot be adjusted, i.e., the maximum value of the window function cannot be changed to a value lower or greater than one. To overcome this limitation, a minor enhancement—adding a multiplicative scale factor to
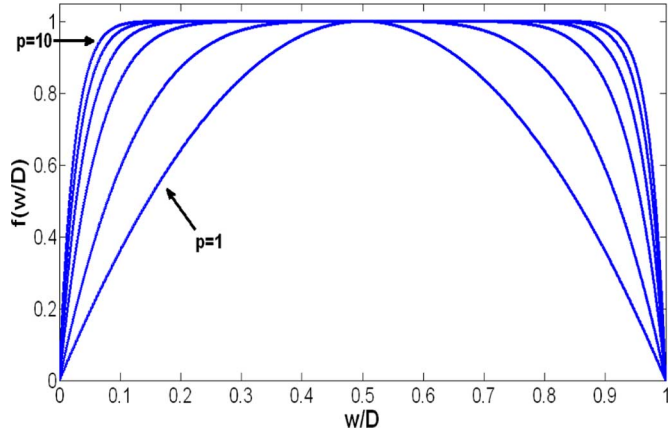
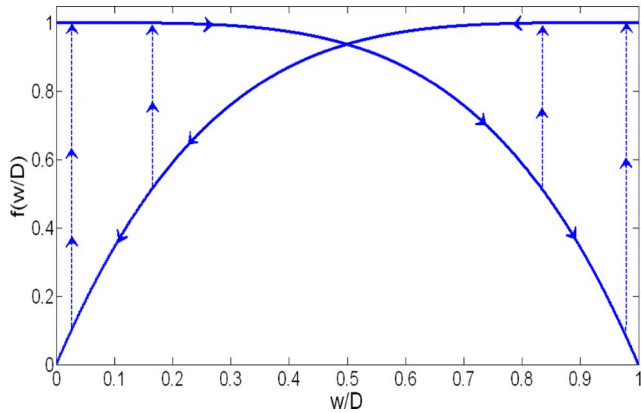Fig. 3. Window function described by (5) according to [12] for several values of p.

Fig. 4. Window function described by (6) according to [13].

Fig. 5. Window function described by (8) according to [14]. (a) Varying p, and (b) varying j.

the window function, has recently been proposed [14]. The proposed window function in [14] is

$$f(w) = j\left(1 - \left[\left(\frac{w}{D} - 0.5\right)^2 + 0.75\right]^p\right), \quad (8)$$

where j is a control parameter which determines the maximum value of $f(w)$ (in this function, the maximum value can be smaller or larger than one). This function is shown in Fig. 5.

While these window functions alleviate the bounds issue and suggest a nonlinear phenomenon, these functions do not exhibit full nonlinear ion drift behavior since the model ignores the nonlinear dependence of the state derivative on the current. A linear ion drift model with a window function does not therefore fully model nonlinear ion drift behavior.

D. Nonlinear Ion Drift Model

While the linear ion drift model is intuitive and satisfies the basic memristive system equations, experiments have shown that the behavior of fabricated memristive devices deviates significantly from this model and is highly nonlinear [15], [16]. The nonlinear I-V characteristic is desirable for logic circuits, and hence more appropriate memristive device models have been proposed. In [17], a model is proposed based on the experi-
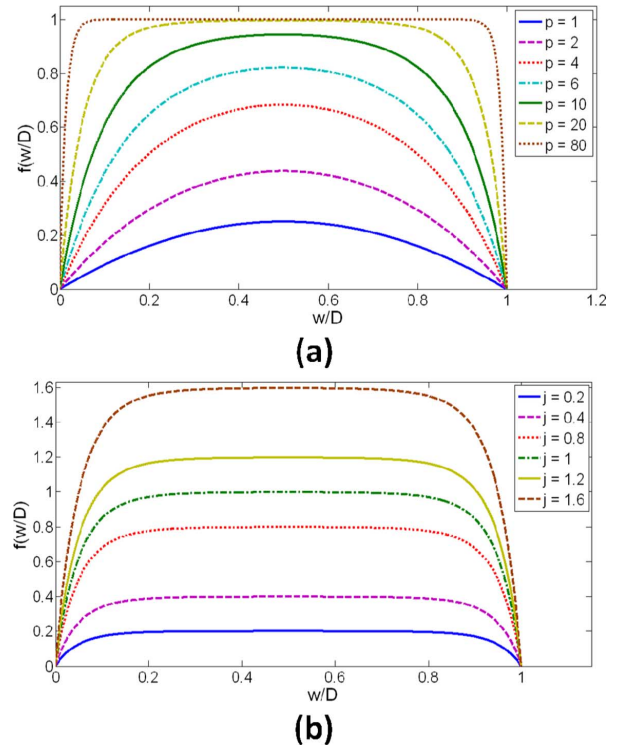
mental results described in [15]. The relationship between the current and voltage is

$$i(t) = w(t)^n \beta \sinh\left(\alpha v(t)\right) + \chi\left[\exp\left(\gamma v(t)\right) - 1\right], \quad (9)$$

where α, β, γ and χ are experimental fitting parameters, and n is a parameter that determines the influence of the state variable on the current. In this model, the state variable w is a normalized parameter within the interval $[0, 1]$. This model assumes an asymmetric switching behavior. When the device is in the ON state, the state variable w is close to one and the current is dominated by the first expression in (9), $\beta \sinh(\alpha v(t))$, which describes a tunneling phenomenon. When the device is in the OFF state, the state variable w is close to zero and the current is dominated by the second expression in (9), $\chi[\exp(\lambda v(t)) - 1]$, which resembles an ideal diode equation.

This model assumes a nonlinear dependence on voltage in the state variable differential equation,

$$\frac{dw}{dt} = a \cdot f(w) \cdot v(t)^m, \quad (10)$$

where a and m are constants, m is an odd integer, and $f(w)$ is a window function. The I-V relationship of a nonlinear ion drift memristive device for sinusoidal and rectangular waveform inputs is illustrated in Fig. 6. A similar model is proposed by the same authors in [28]. In this model, the same I-V relationship is described with a more complex state drift derivative.

E. Simmons Tunnel Barrier Model

Linear and nonlinear ion drift models are based on representing the two regions of oxide and doped oxide as two resis-
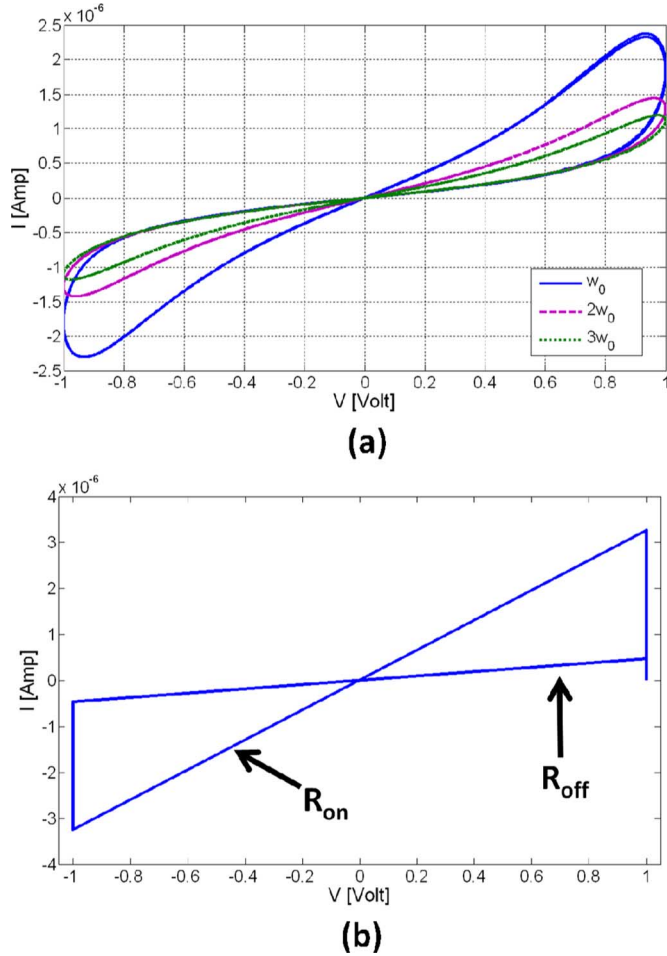
(a)

(b)

Fig. 6. Nonlinear ion drift model I-V curve. $m = 5$, $n = 2$, $a = 1\,\mathrm{V}^{-m}\mathrm{s}^{-1}$, $\beta = 0.9\,\mu\mathrm{A}$, $\gamma = 4\,\mathrm{V}^{-1}$, $\chi = 10^{-4}\,\mu\mathrm{A}$, and $\alpha = 2\,\mathrm{V}^{-1}$. (a) Sinusoidal voltage input for several frequencies ω_0, $2\omega_0$, and $3\omega_0$, and (b) rectangular waveform of input voltage.
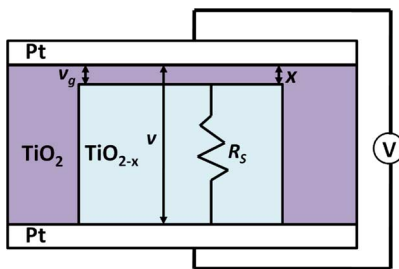

Fig. 7. Physical model of Simmons tunnel barrier memristive device. The state variable x is the width of the oxide region, V is the applied voltage on the device, v_g is the voltage in the undoped region, and v is the internal voltage in the device.

tors in series. A more accurate physical model was proposed in [18]. This model assumes nonlinear and asymmetric switching behavior due an exponential dependence of the movement of the ionized dopants, namely, changes in the state variable. In this model, rather than two resistors in series as in the linear drift model, there is a resistor in series with an electron tunnel barrier, as shown in Fig. 7. The state variable x is the Simmons tunnel barrier width [19] (note that a different notation for the state variable is used to prevent confusion with the role of the state variable in the linear ion drift model). In this case, the derivative
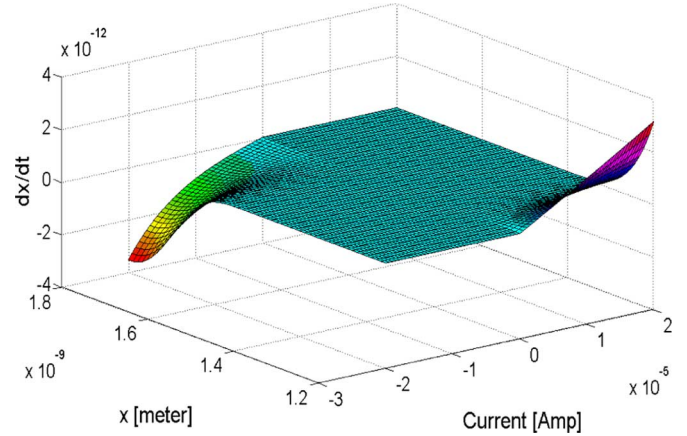

Fig. 8. Derivative of the state variable x as described in (11). The fitting parameters are $c_{off} = 3.5\,\mu\mathrm{m/s}$, $i_{off} = 115\,\mu\mathrm{A}$, $a_{off} = 1.2\,\mathrm{nm}$, $c_{on} = 40\,\mu\mathrm{m/s}$, $i_{on} = 8.9\,\mu\mathrm{A}$, $a_{on} = 1.8\,\mathrm{nm}$, $b = 500\,\mu\mathrm{A}$, and $w_c = 107\,\mathrm{pm}$.

of x can be interpreted as the oxygen vacancy drift velocity, and is

$$\frac{dx(t)}{dt} = \begin{cases} c_{off} \sinh\left(\dfrac{i}{i_{off}}\right) \exp\left[-\exp\left(\dfrac{x-a_{off}}{w_c} - \dfrac{|i|}{b}\right) - \dfrac{x}{w_c}\right], & i > 0 \quad (11\mathrm{a}) \\[2ex] c_{on} \sinh\left(\dfrac{i}{i_{on}}\right) \exp\left[-\exp\left(-\dfrac{x-a_{on}}{w_c} - \dfrac{|i|}{b}\right) - \dfrac{x}{w_c}\right], & i < 0, \quad (11\mathrm{b}) \end{cases}$$

where c_{off}, c_{on}, i_{off}, i_{on}, a_{off}, a_{on}, w_c, and b are fitting parameters. Equation (11) is illustrated in Fig. 8 for the measured fitting parameters reported in [18]. The physical phenomena behind the behavior shown in (11) are not yet fully understood, but considered to be a mixture of nonlinear drift at high electric fields and local Joule heating enhancing the oxygen vacancies. In practical memristive devices, the ON switching is significantly faster than the OFF switching because of the diffusion of the oxygen vacancies from TiO_{2-x} to TiO_2, and the drift of the oxygen vacancies due to the internal electric field is different for positive and negative voltages. For a negative voltage (lower x), the drift of the oxygen vacancies and the diffusion are in the same direction, while for a positive voltage, the direction of diffusion and drift is opposite [20]. The parameters c_{off} and c_{on} influence the magnitude of the change of x. The parameter c_{on} is an order of magnitude larger than the parameter c_{off}. The parameters i_{off} and i_{on} effectively constrain the current threshold. Below these currents, the change in the derivative of x is neglected. A current threshold phenomenon is desirable for digital applications. The parameters a_{off} and a_{on} force, respectively, the upper and lower bounds for x. Because of the exponential dependence on $x - a_{off}$ or $x - a_{on}$, the derivative of the state variable is significantly smaller for the state variable within the permitted range. There is therefore no need for a window function in this model.

In this model, the relationship between the current and voltage is shown as an implicit equation based on the Simmons tunneling model [19],

$$\begin{aligned} i(t) = {} & \tilde{A}(x, v_g) \phi_1(v_g, x) \exp\left(-B(v_g, x) \cdot \phi_1(v_g, x)^{1/2}\right) \\ & - \tilde{A}(x, v_g) \left(\phi_1(v_g, x) + e|v_g|\right) \\ & \times \exp\left(-B(v_g, x) \cdot (\phi_1(v_g, x) + ev_g)^{1/2}\right), \quad (12) \end{aligned}$$
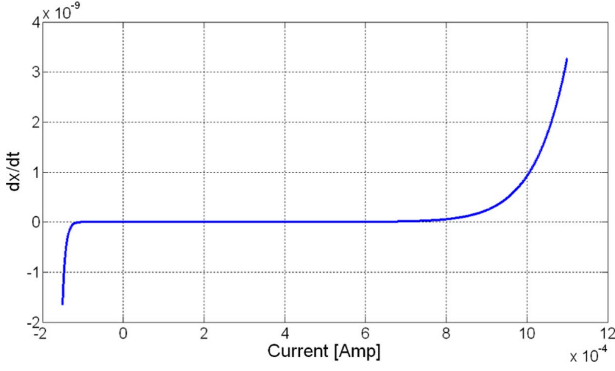
$$v_g = v - i(t)R_s, \quad (13)$$

Fig. 9. Derivative of the state variable x as described in (11) under the assumption of a small change in $x(x \sim 1.5 \text{ nm})$. Note that the device exhibits a threshold current. The same fitting parameters as used in Fig. 8 are used.

where v is the internal voltage on the device, which is not necessarily equal to the applied voltage on the device V (i.e., the external voltage V and the internal voltage v are not necessarily the same [18]).

IV. THRESHOLD ADAPTIVE MEMRISTOR (TEAM) MODEL

In this section, TEAM, a novel memristive device model, is presented. The integral portion of the TEAM model is based on an expression for the derivative of the internal state variable that can be fitted to any memristive device type. Unlike other memristive device models, the current-voltage relationship is undefined and can be freely chosen from any current-voltage relationship. Several examples of possible current-voltage relationships are described in Section IV-B. This relationship is not limited to these examples. In Section IV-A, the disadvantages of the aforementioned models and the need for such a model are explained. The derivative of the internal state variable of the memristive device [the relevant expression for (1)] and examples of the current-voltage relationship [the relevant expression for (2)] are described, respectively, in Section IV-B and IV-C. Proper fitting of the Simmons tunnel barrier model to the TEAM model is presented in Section IV-D, as well as the proper window function for this fitting.

A. Need for a Simplified Model

The Simmons tunnel barrier model is, to the authors' best knowledge, the most accurate physical model of a TiO_2 memristive device. This model is however quite complicated, without an explicit relationship between current and voltage, and not general in nature (i.e., the model fits only a specific type of memristive device). A complex SPICE model of the Simmons tunnel barrier model is presented in [21]. This model is also computational inefficient. A model with simpler expressions rather than the complex equations in the Simmons tunnel barrier model is therefore desired. Yet the accuracy of the simple model must be adequate. This simplified model represents the same physical behavior, but with simpler mathematical functions. In Section V, simplifying assumptions are introduced. Namely, no change in the state variable is assumed below a certain threshold, and a polynomial dependence rather than an exponential dependence is used. These assumptions

are applied to support simple analysis and computational efficiency.

B. State Variable Derivative in TEAM Model

Note in Fig. 9 and (11) that because of the high nonlinear dependence of the memristive device current, the memristive device can be modeled as a device with threshold currents. This approximation is similar to the threshold voltage approximation in MOS transistors. This approximation is justified, since for small changes in the electric tunnel width, separation of variables can be performed. The dependence of the internal state derivative on current and the state variable itself can be modeled as independently multiplying two independent functions; one function depends on the state variable x and the other function depends on the current.

Under these assumptions, the derivative of the state variable for the simplified proposed model is

$$
\frac{dx(t)}{dt} = \begin{cases} k_{off} \cdot \left(\dfrac{i(t)}{i_{off}} - 1 \right)^{\alpha_{off}} \cdot f_{off}(x), & 0 < i_{off} < i \quad \text{(14a)} \\ 0, & i_{on} < i < i_{off} \quad \text{(14b)} \\ k_{on} \cdot \left(\dfrac{i(t)}{i_{on}} - 1 \right)^{\alpha_{on}} \cdot f_{on}(x), & i < i_{on} < 0, \quad \text{(14c)} \end{cases}
$$

where k_{off}, k_{on}, α_{off}, and α_{on} are constants, i_{off} and i_{on} are current thresholds, and x is the internal state variable, which represents the effective electric tunnel width. The constant parameter k_{off} is a positive number, while the constant parameter k_{on} is a negative number. The functions $f_{off}(x)$ and $f_{on}(x)$ represent the dependence on the state variable x. These functions behave as the window functions described in Section II, which constrain the state variable to bounds of $x \in [x_{on}, x_{off}]$. Alternatively, these functions can be different functions of x. The functions $f_{on}(x)$ and $f_{off}(x)$ are not necessarily equal, since the dependence on x may be asymmetric (as in the Simmons tunnel barrier model). Note that the role of x in this model is opposite to w in the linear ion drift model.

C. Current—Voltage Relationship in TEAM Model

Assume the relationship between the voltage and current of a memristive device is similar to (4). The memristance changes linearly in x, and (2) becomes

$$
v(t) = \left[R_{ON} + \frac{R_{OFF} - R_{ON}}{x_{off} - x_{on}} (x - x_{on}) \right] \cdot i(t). \quad \text{(15)}
$$

The reported change in the resistance however is an exponential dependence on the state variable [18], since the memristance, in practical memristive devices, is dependent on a tunneling effect, which is highly nonlinear. If (12) describes the current-voltage relationship in the model, the model becomes inefficient in terms of computational time and is also not general. Therefore, any change in the tunnel barrier width changes the memristance, and is assumed to change in an exponential manner. Under this assumption, (2) becomes

$$
v(t) = R_{ON} e^{(\lambda / x_{off} - x_{on})(x - x_{on})} \cdot i(t), \quad \text{(16)}
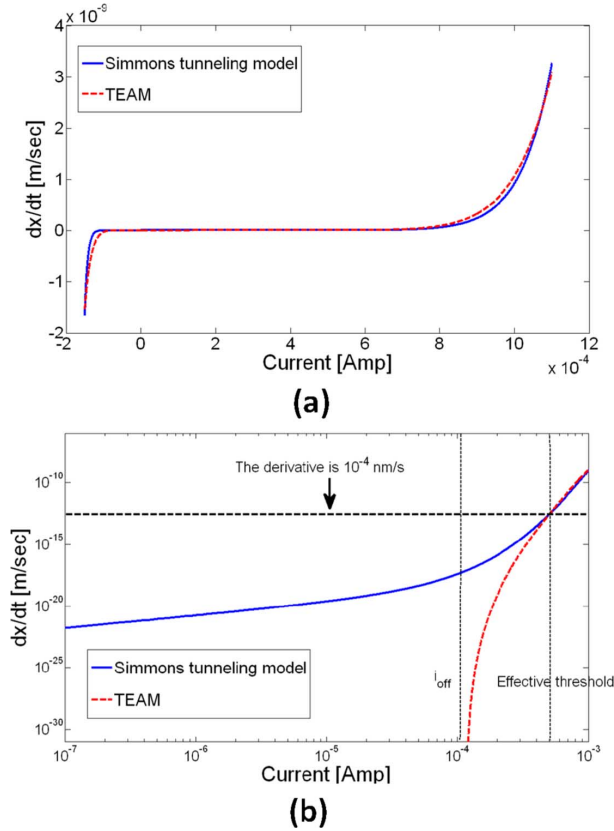$$

(a)

(b)

Fig. 10. Fitting between the derivative of the state variable x in the Simmons tunnel barrier memristive device model and the TEAM model. The same fitting parameters as used in Fig. 8 are used for the Simmons tunnel barrier model. (a) The fitting parameters for the proposed model are $k_{off} = 1.46e\text{-}9$ nm/s, $\alpha_{off} = 10$, $i_{off} = 115\,\mu A$, $k_{on} = -4.68e\text{-}13$ nm/s, $\alpha_{on} = 10$, and $i_{on} = 8.9\,\mu A$. (b) Fitting procedure in a logarithmic scale. The operating current range is assumed to be $0.1\,\mu A$ to 1 mA and the neglected value for the derivative of the state variable is assumed to be 10^{-4} nm/s. For any desired current range, the proper fitting parameters can be evaluated to maintain an accurate match between the models. For the aforementioned parameters, a reasonable current threshold is 0.5 mA (marked as the effective threshold in the figure).

where λ is a fitting parameter, and R_{ON} and R_{OFF} are the equivalent effective resistance at the bounds, similar to the notation in the linear ion drift model, and satisfy

$$\frac{R_{OFF}}{R_{ON}} = e^{\lambda}. \qquad (17)$$

D. Fitting the Simmons Tunnel Barrier Model to the TEAM Model

The TEAM model is inspired by the Simmons tunnel barrier model. However, to use this model for practical memristive devices, similar to the Simmons tunnel barrier model, a fit to the TEAM model needs to be accomplished. Since (14) is derived from a Taylor series, for any desired range of memristive device current, λ, k_{off}, k_{on}, α_{off}, and α_{on} can be evaluated to achieve a sufficiently accurate match between the models. As the desired operating current range for the memristive device is wider, to maintain sufficiently accuracy, the required α_{off} and α_{on} are higher, thereby increasing the computational time. The proper fitting procedure to the current threshold is to plot the derivative of the exact state variable in the actual operating range of the current, and decide what value of the state variable derivative is effectively zero (i.e., the derivative of the state variable is
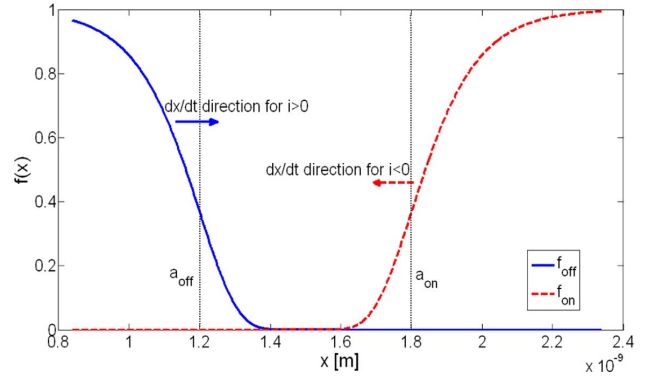

Fig. 11. Proposed $f_{on}(x)$ and $f_{off}(x)$ based on (18) and (19). These functions represent the dependence on x in (14) and also force bounds for x since $f_{off}(x)$ is used when dx/dt is positive and is zero around a_{on}, and vice versa for $f_{on}(x)$.

significantly smaller and can therefore be neglected). The current at this effective point is a reasonable value of the current threshold. In this paper, the parameters i_{on} and i_{off} are chosen as these current thresholds, since these terms represent the exponential dependence of the derivative on the state variable of the current in the Simmons tunnel barrier model. A fit of the Simmons tunnel barrier model to the TEAM model is shown in Fig. 10(a). The proper current threshold fitting procedure is shown in Fig. 10(b). Note that a reasonable current threshold can be higher than i_{off}.

As mentioned in Section IV-B, the functions $f_{off}(x)$ and $f_{on}(x)$ are window functions, or alternatively, functions that fit the Simmons tunnel barrier model based upon the separation of variables of (11). These functions represent the dependence of the derivative in the state variable x. Based on the fitting parameters reported in [18], possible functions $f_{off}(x)$ and $f_{on}(x)$ are, respectively,

$$f_{off}(x) = \exp\left[-\exp\left(\frac{x - a_{off}}{w_c}\right)\right], \qquad (18)$$

$$f_{on}(x) = \exp\left[-\exp\left(-\frac{x - a_{on}}{w_c}\right)\right]. \qquad (19)$$

The determination process for (18) and (19) is presented in Appendix A. Note that (18) and (19) maintain the limitation of certain bounds for the state variable x since the derivative of x around a_{on} when using (18) and (19) is effectively zero for positive current (f_{off} is practically zero) and negative for negative current. x can only be reduced. The value of x can be increased for values of x around a_{off}. Therefore, a reasonable value for the state variable bounds x_{on} and x_{off} is, respectively, a_{off} and a_{on}. Although the proposed function limits the bounds of the state variable, there is no problem when the bounds are exceeded, unlike other window functions. This characteristic is useful for simulations, where the bounds can be exceeded due to the discrete nature of simulation engines. The proposed terms, f_{off} and f_{on}, are illustrated in Fig. 11.

The I-V relationship and state variable behavior of the proposed model are shown in Figs. 12 and 13 for an ideal rectangular window function and the proposed window function. Note in Figs. 12 and 13 that there is a performance difference between the different window functions. Due to the significant nonlinearity, the proposed window function constrains the state
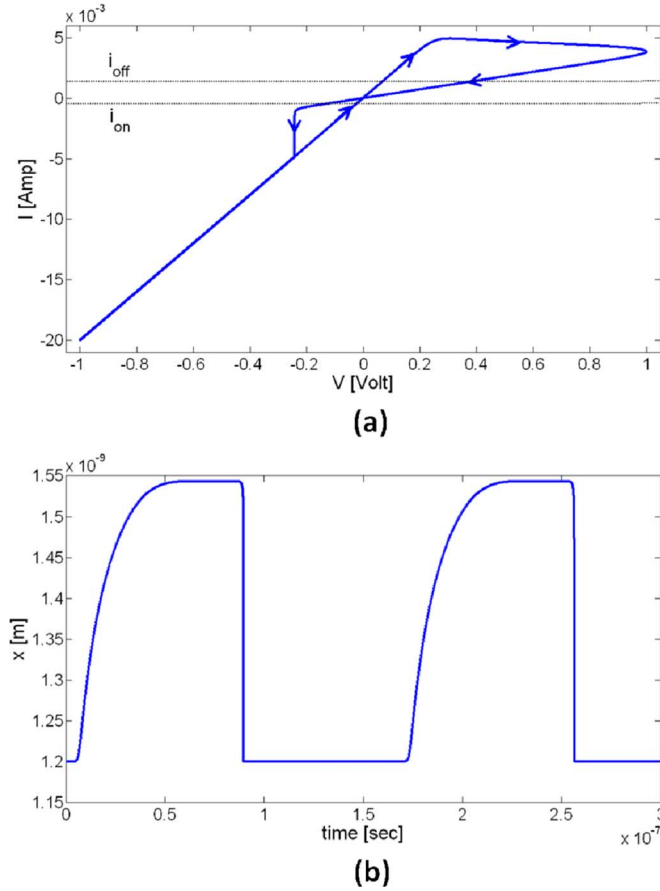
Fig. 12. The TEAM model driven with a sinusoidal input of 1 volt using the same fitting parameters as used in Fig. 10, $R_{ON} = 50\,\Omega$, $R_{OFF} = 1$ kΩ, and an ideal rectangular window function for $f_{on}(x)$ in (19) and $f_{off}(x)$ in (18). (a) I-V curve, and (b) state variable x. Note that the device is asymmetric, i.e., switching OFF is slower than switching ON.

variable to a small range, and the memristive devices are activated within a significantly smaller time scale as compared to an ideal rectangular window function. The required conditions for a sufficient fit of the TEAM model to the Simmons tunnel barrier model, as described in Appendix A, cannot be maintained for a symmetric input voltage due to the asymmetry of the Simmons tunnel model. The required conditions for a sufficient fit are therefore not maintained in Fig. 13. These conditions are however maintained in Fig. 14, where the behavior of the TEAM model and the Simmons tunnel barrier model is compared and exhibits excellent agreement. While the proposed model fits the Simmons Tunnel Barrier model, the TEAM model is general and flexible. The model can fit different physical memristive device models, including other types of memristive devices, such as STT-MRAM and Spintronic memristors [6], [24].

V. COMPARISON BETWEEN THE MODELS

A comparison between the different memristive device models is listed in Table I and a comparison between different window functions is listed in Table II. A comparison of the accuracy and complexity between the Simmons tunnel barrier memristive device and TEAM models is shown in Fig. 14. The TEAM model can improve the simulation runtime by 47.5% and is sufficiently accurate, with a mean error of 0.2%. These results are dependent on the particular TEAM parameters. A lower value for α_{ON} and α_{OFF} produces lower accuracy and
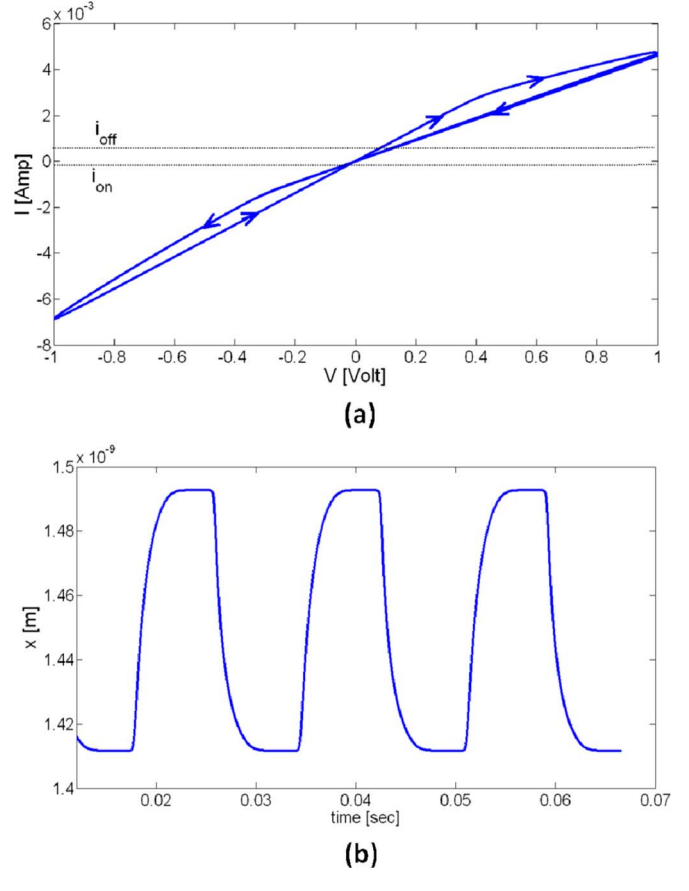

Fig. 13. The TEAM model driven with a sinusoidal input of 1 volt using the same fitting parameters as used in Fig. 10, $R_{ON} = 50\,\Omega$, $R_{OFF} = 1$ kΩ, proposed $f_{on}(x)$ in (19), and $f_{off}(x)$ in (18) with the same parameters used in Fig. 8. (a) I-V curve, and (b) state variable x. Note that the device is asymmetric, i.e., switching OFF is slower than switching ON.

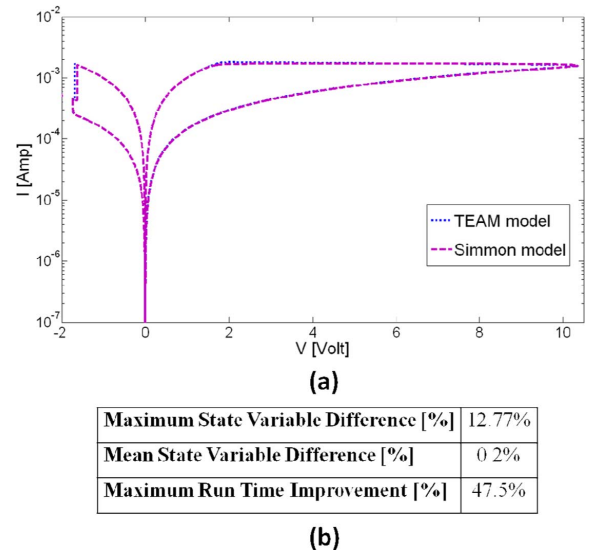| Maximum State Variable Difference [%]	12.77%
Mean State Variable Difference [%]	0.2%
Maximum Run Time Improvement [%]	47.5%

(b)

Fig. 14. TEAM model fitted to Simmons tunnel barrier model. (a) I-V curve for both models, and (b) fitting accuracy in terms of internal state variable x and maximum improvement in runtime for MATLAB simulations. The state variable average and maximum differences are, respectively, 0.2% and 12.77%. The TEAM fitting parameters are $R_{ON} = 1$ kΩ, $R_{OFF} = 100$ kΩ, $k_{on} = 4.13e\text{-}33$ nm/s, $\alpha_{on} = 25$, $k_{off} = 4.13e\text{-}33$ nm/s, $\alpha_{off} = 25$, $i_{off} = 115\,\mu$A, and $i_{on} = 8.9\,\mu$A.

enhanced computational runtime. The TEAM model satisfies the primary equations of a memristive system as described in

TABLE I
COMPARISON OF DIFFERENT MEMRISTIVE DEVICE MODELS

Model	Linear ion drift [3]	Nonlinear ion drift [17]	Simmons tunneling barrier [18]	Yakopcic *et al* [25]	TEAM
State variable	$0 \leq w \leq D$ Doped region physical width	$0 \leq w \leq 1$ Doped region normalized width	$a_{off} \leq x \leq a_{on}$ Undoped region width	$0 \leq x \leq 1$ No physical explanation	$x_{on} \leq x \leq x_{off}$ Undoped region width
Control mechanism	Current controlled	Voltage controlled	Current controlled	Voltage controlled	Current controlled
Current-voltage relationship and memristance deduction	Explicit	I-V relationship – explicit Memristance deduction - ambiguous	Ambiguous	Ambiguous	Explicit
Matching memristive system definition	Yes	No	No	No	Yes
Generic	No	No	No	Moderate	Yes
Accuracy comparing practical memristive devices	Lowest accuracy	Low accuracy	Highest accuracy	Moderate accuracy	Sufficient accuracy
Threshold exists	No	No	Practically exists	Yes	Yes

TABLE II
COMPARISON OF DIFFERENT WINDOW FUNCTIONS

Function	Joglekar [12]	Biolek [13]	Prodromakis [14]	TEAM
$f(x)/f(w)$	$f(w) = 1-(2w/D-1)^{2p}$	$f(w) = 1-(w/D-stp(-i))^{2p}$	$f(w)=j(1-[(w-0.5)^2+0.75]^p)$	$f_{on,off}=\exp[-\exp(|x-x_{on,off}|/w_c)]$
Symmetric	Yes	Yes	Yes	Not necessarily
Resolve boundary conditions	No	Yes	Practically yes	Practically yes
Impose nonlinear drift	Partially	Partially	Partially	Yes
Scale factor $f_{max} < 1$	No	No	Yes	No
Fits memristive device model	Linear/nonlinear ion drift/TEAM	Linear/nonlinear ion drift/TEAM	Linear/nonlinear ion drift/TEAM	TEAM for Simmons tunneling barrier fitting

(1) and (2), and the convergence conditions and computational efficiency required by simulation engines.

The TEAM model accurately characterizes not only the Simmons tunnel barrier model, but also a variety of different models. For example, the TEAM model can be fitted to the linear ion drift behavior, where

$$k_{on} = k_{off} = \mu_v \frac{R_{ON}}{D} i_{on}, \tag{20}$$

$$\alpha_{on} = \alpha_{off} = 1, \tag{21}$$

$$i_{on} = i_{off} \rightarrow 0, \tag{22}$$

$$x_{on} = D, \tag{23}$$

$$x_{off} = 0, \tag{24}$$

$$x = D - w. \tag{25}$$

To include memristive devices into the circuit design process, these models need to be integrated into a CAD environment, such as SPICE. There are several proposed SPICE macromodels for the linear ion drift model [13], [22] and the nonlinear ion drift model [17]. A SPICE model for the Simmons tunneling barrier model has recently been proposed [21], but is complicated and inefficient in terms of computational time. Another simplified model has recently been proposed, assuming voltage threshold and an implicit memristance [25]. In this model, the current and voltage are related through a hyperbolic sine and the derivative of the state variable is an exponent. This model is less general than the TEAM model and more complex in terms of computational time (the model uses sinh and exponents rather than poly-

nomials as in the TEAM model). The model is also less accurate than the TEAM model when fitting the model to the Simmons tunnel barrier model.

The TEAM model can be described in a SPICE macromodel similar to the proposed macromodel in [23], as shown in Fig. 15. In this macromodel, the internal state variable is represented by the voltage across the capacitor C and the bounds of the state variable are enforced by diodes $D1$ and $D2$. A Verilog-A model is however chosen because it is more efficient in terms of computational time than a SPICE macromodel, while providing similar accuracy. A Verilog-A form of the model, as described in this paper, has been implemented. The code for these models can be found in [26]. Although the state variable derivative in the TEAM model is not a smooth function, it is a continuous function based only on polynomial functions. The Verilog-A model has been tested in complex simulations (hundreds of memristive devices) and did not exhibit any convergence issues.

VI. CONCLUSIONS

Different memristive device models are described in this paper—linear ion drift, nonlinear ion drift, Simmons tunnel barrier, and TEAM (ThrEshold Adaptive Memristor), as well as different window functions. The TEAM model is a flexible and convenient model that can be used to characterize a variety of different practical memristive devices. This model suggests a memristive device should exhibit a current threshold and nonlinear dependence on the charge, as well as a dependence on the state variable.
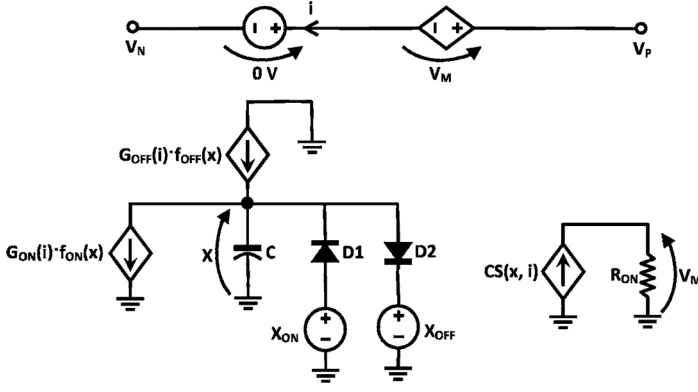
Fig. 15. TEAM SPICE macromodel. The state variable x is the voltage across the capacitor $C = 1$ F. The initial voltage is the initial state variable. $D1$ and $D2$ constrain the bounds of the state variable to the value of the voltage sources x_{ON} and x_{OFF}. $G_{ON}(i)$ and $G_{OFF}(i)$ are the relevant functions from (14). $CS(x, i)$ is determined from the current-voltage relationship, and is $i \cdot \exp[\lambda(x - x_{on})/(x_{off} - x_{on})]$ for the current-voltage relationship in (16). V_N and V_P are, respectively, the negative and positive ports of the memristive device, and i is the memristive device current.

A comparison between the TEAM model and other memristive device models is presented. The TEAM model is simple, flexible, and general. While the simplicity of this model improves the efficiency of the simulation process, the model is sufficiently accurate, exhibiting an average error of only 0.2% as compared to the Simmons tunnel barrier state variable. This model fits practical memristive devices better than previously proposed models. This model is suitable for memristive device-based circuit design and has been implemented in Verilog-A for SPICE simulations.

APPENDIX
APPROPRIATE FITTING WINDOW FUNCTION TO THE SIMMONS TUNNEL BARRIER MODEL

The purpose of this appendix is to determine a proper window function $f(x)$ that provides a sufficient fit to the Simmons tunnel barrier model. To determine a reasonable approximation, parameter values from [18] are used. From (11a) and (11b), the derivative of the state variable x is

$$\frac{dx(t)}{dt} = \begin{cases} C_{off} \sinh\left(\dfrac{i}{i_{off}}\right)\exp\left[-\exp\left(\dfrac{x-a_{off}}{w_c}-\dfrac{|i|}{b}\right)-\dfrac{x}{w_c}\right], & i>0 \quad \text{(A.1.a)} \\ C_{on} \sinh\left(\dfrac{i}{i_{on}}\right)\exp\left[-\exp\left(-\dfrac{x-a_{on}}{w_c}-\dfrac{|i|}{b}\right)-\dfrac{x}{w_c}\right], & i<0. \quad \text{(A.1.b)} \end{cases}$$

The derivative of the state variable is a multiplicand of two functions—a hyperbolic sine function which depends only on the current and an exponential function which depends on both the current and the state variable. To simplify (A.1) and to apply separation of variables, approximations

$$\frac{x-a_{off}}{w_c} \gg \frac{|i|}{b} \tag{A.2.a}$$

$$\frac{a_{on}-x}{w_c} \gg \frac{|i|}{b} \tag{A.2.b}$$

need to be assumed. In this appendix, the range of the required state variable for this approximation is determined. From (A.1), an approximation for $f(x)$ is provided.

The Simmons tunnel barrier model is appropriate when the state variable x is limited by a_{off} and a_{on}, i.e.,

$$a_{off} \leq x \leq a_{on}. \tag{A.3}$$

From the parameters in [18],

$$0 \leq \frac{x-a_{off}}{w_c} \leq \frac{a_{on}-a_{off}}{w_c} = \frac{1.8\mu-1.2\mu}{107p} \approx \frac{600n}{0.1n} = 6\cdot10^3 \Rightarrow$$

$$0 \leq \frac{x-a_{off}}{w_c} \leq 6\cdot10^3$$

$$0 \leq \frac{a_{on}-x}{w_c} \leq 6\cdot10^3 \tag{A.4}$$

Assume the maximum current in the device is 100 μA,

$$0 \leq \frac{|i|}{b} \leq \frac{100\mu}{500\mu} = \frac{1}{5}. \tag{A.5}$$

Assume that the value of the state variable is one of the effective boundaries a_{on} and a_{off},

$$x \approx a_{on} \Rightarrow \frac{1}{5} \ll \frac{x-a_{off}}{w_c} \leq 6000$$

$$\Rightarrow \frac{x-a_{off}}{w_c} - \frac{|i|}{b} \approx \frac{x-a_{off}}{w_c}$$

$$x \approx a_{off} \Rightarrow \frac{1}{5} \ll \frac{a_{on}-x}{w_c} \leq 6000$$

$$\Rightarrow \frac{a_{on}-x}{w_c} - \frac{|i|}{b} \approx \frac{a_{on}-x}{w_c} \tag{A.6}$$

To maintain the same approximation as in (A.6), it is sufficient to assume that the value of the expression in (A.5) is relatively small. Assume that one order of magnitude is sufficient for this assumption. The proper range of x can be determined as

$$\frac{|i|}{b} \leq \frac{1}{5} \ll 2 \leq \frac{x-a_{off}}{w_c} \Rightarrow 2w_c + a_{off} \leq x \tag{A.7}$$

$$\frac{|i|}{b} \leq \frac{1}{5} \ll 2 \leq \frac{a_{on}-x}{w_c} \Rightarrow x \leq a_{on} - 2w_c \tag{A.8}$$

For positive current, the derivative of x is positive and therefore the value of x is increasing. It is reasonable to assume (A.8). Similarly, for negative current, it is reasonable to assume (A.7). Under these assumptions, separation of variables can be achieved. See (A.9) at the top of the next page.

Based on the parameters in [18] and the exponential dependence, the exponential term is significantly greater than the second term,

$$x \approx a_{on}$$

$$\Rightarrow \exp\left(\frac{x-a_{off}}{w_c}\right) \approx \exp\left(\frac{a_{on}-a_{off}}{w_c}\right)$$

$$\approx \exp(6000) \gg \frac{x}{w_c} \approx \frac{a_{on}}{w_c} \approx 20$$

$$\Rightarrow \exp\left(\frac{x-a_{off}}{w_c}\right) \gg \frac{x}{w_c} \tag{A.10}$$

And similarly,

$$x \approx a_{off} \Rightarrow \exp\left(-\frac{x-a_{on}}{w_c}\right) \gg \frac{x}{w_c} \tag{A.11}$$

$$\frac{dx(t)}{dt} = \begin{cases} f_{off} \sinh\left(\frac{i}{i_{off}}\right) \exp\left[-\exp\left(\frac{x-a_{off}}{w_c} - \frac{|i|}{b}\right) - \frac{x}{w_c}\right], & i > 0 \\ f_{on} \sinh\left(\frac{i}{i_{on}}\right) \exp\left[-\exp\left(-\frac{x-a_{on}}{w_c} - \frac{|i|}{b}\right) - \frac{x}{w_c}\right], & i < 0 \end{cases}$$

$$\underset{\substack{i<0,\, x\approx a_{off} \\ i>0,\, x\approx a_{on}}}{\Rightarrow} \approx \begin{cases} f_{off} \sinh\left(\frac{i}{i_{off}}\right) \exp\left[-\exp\left(\frac{x-a_{off}}{w_c}\right) - \frac{x}{w_c}\right], & i > 0 \\ f_{on} \sinh\left(\frac{i}{i_{on}}\right) \exp\left[-\exp\left(-\frac{x-a_{on}}{w_c}\right) - \frac{x}{w_c}\right], & i < 0 \end{cases}$$

$$\Rightarrow \frac{dx(t)}{dt} = g(i) \cdot f(x)$$

$$\Rightarrow f(x) = \begin{cases} \exp\left[-\exp\left(\frac{x-a_{off}}{w_c}\right) - \frac{x}{w_c}\right], & i > 0 \\ \exp\left[-\exp\left(-\frac{x-a_{on}}{w_c}\right) - \frac{x}{w_c}\right], & i < 0 \end{cases} \tag{A.9}$$

From (A.10) and (A.11), the proposed window function is therefore

$$f_{on}(x) = \exp\left[-\exp\left(-\frac{x-a_{on}}{w_c}\right)\right] \tag{A.12}$$

$$f_{off}(x) = \exp\left[-\exp\left(\frac{x-a_{off}}{w_c}\right)\right] \tag{A.13}$$

Acknowledgment

References

[1] L. O. Chua, "Memristor—The missing circuit element," *IEEE Trans. Circuit Theory*, vol. CT-18, no. 5, pp. 507–519, Sep. 1971.

[2] L. O. Chua and S. M. Kang, "Memristive devices and systems," *Proc. IEEE*, vol. 64, no. 2, pp. 209–223, Feb. 1976.

[3] D. B. Strukov, G. S. Snider, D. R. Stewart, and R. S. Williams, "The missing memristor found," *Nature*, vol. 453, pp. 80–83, May 2008.

[4] D. Sacchetto, M. H. Ben-Jamaa, S. Carrara, G. DeMicheli, and Y. Leblebici, "Memristive devices fabricated with silicon nanowire schottky barrier transistors," in *Proc. IEEE Int. Symp. Circuits Syst.*, May/Jun. 2010, pp. 9–12.

[5] K. A. Campbell, A. Oblea, and A. Timilsina, "Compact method for modeling and simulation of memristor devices: Ion conductor chalcogenide-based memristor devices," in *Proc. IEEE/ACM Int. Symp. Nanoscale Archit.*, Jun. 2010, pp. 1–4.

[6] X. Wang, Y. Chen, H. Xi, and D. Dimitrov, "Spintronic memristor through spin-torque-induced magnetization motion," *IEEE Electron Device Lett.*, vol. 30, no. 3, pp. 294–297, Mar. 2009.

[7] Y. Ho, G. M. Huang, and P. Li, "Nonvolatile memristor memory: Device characteristics and design implications," in *Proc. IEEE Int. Conf. Comput.-Aided Design*, Nov. 2009, pp. 485–490.

[8] A. Afifi, A. Ayatollahi, and F. Raissi, "Implementation of biologically plausible spiking neural network models on the memristor crossbar-based CMOS/Nano circuits," in *Proc. Eur. Conf. Circuit Theory Design*, Aug. 2009, pp. 563–566.

[9] Y. V. Pershin and M. Di Ventra, "Practical approach to programmable analog circuits with memristors," *IEEE Trans. Circuits Syst. I, Reg. Papers*, vol. 57, no. 8, pp. 1857–1864, Aug. 2010.

[10] G. Snider, "Computing with hysteretic resistor crossbars," *Appl. Phys. A, Mater. Sci. Process.*, vol. 80, no. 6, pp. 1165–1172, Mar. 2005.

[11] Z. Diao, Z. Li, S. Wang, Y. Ding, A. Panchula, E. Chen, L. C. Wang, and Y. Huai, "Spin-transfer torque switching in magnetic tunnel junctions and spin-transfer torque random access memory," *J. Phys., Condens. Matter*, vol. 19, no. 16, pp. 1–13, Apr. 2007.

[12] Y. N. Joglekar and S. J. Wolf, "The elusive memristor: Properties of basic electrical circuits," *Eur. J. Phys.*, vol. 30, no. 4, pp. 661–675, Jul. 2009.

[13] Z. Biolek, D. Biolek, and V. Biolkova, "SPICE model of memristor with nonlinear dopant drift," *Radioengineering*, vol. 18, no. 2, pt. 2, pp. 210–214, Jun. 2009.

[14] T. Prodromakis, B. P. Peh, C. Papavassiliou, and C. Toumazou, "A versatile memristor model with non-linear dopant kinetics," *IEEE Trans. Electron Devices*, vol. 58, no. 9, pp. 3099–3105, Sep. 2011.

[15] J. J. Yang, M. D. Pickett, X. Li, D. A. A. Ohlberg, D. R. Stewart, and R. S. Williams, "Memristive switching mechanism for metal/oxide/metal nanodevices," *Nature Nanotechnol.*, vol. 3, pp. 429–433, Jul. 2008.

[16] D. B. Strukov and R. S. Williams, "Exponential ionic drift: Fast switching and low volatility of thin-film memristors," *Appl. Phys. A, Mater. Sci. Process.*, vol. 94, no. 3, pp. 515–519, Mar. 2009.

[17] E. Lehtonen and M. Laiho, "CNN using memristors for neighborhood connections," in *Proc. Int. Workshop Cell. Nanoscale Netw. Their Appl.*, Feb. 2010, pp. 1–4.

[18] M. D. Pickett, D. B. Strukov, J. L. Borghetti, J. J. Yang, G. S. Snider, D. R. Stewart, and R. S. Williams, "Switching dynamics in titanium dioxide memristive devices," *J. Appl. Phys.*, vol. 106, no. 7, pp. 1–6, Oct. 2009.

[19] J. G. Simmons, "Generalized formula for the electric tunnel effect between similar electrodes separated by a thin insulating film," *J. Appl. Phys.*, vol. 34, no. 6, pp. 1793–1803, Jan. 1963.

[20] D. B. Strukov, J. L. Borghetti, and R. S. Williams, "Coupled ionic and electronic transport model of thin-film semiconductor memristive behavior," *Small*, vol. 5, no. 9, pp. 1058–1063, May 2009.

[21] H. Abdalla and M. D. Pickett, "SPICE modeling of memristors," in *IEEE Int. Symp. Circuits Syst.*, May 2011, pp. 1832–1835.

[22] S. Benderli and T. A. Wey, "On SPICE macromodelling of TiO_2 memristors," *Electron. Lett.*, vol. 45, no. 7, pp. 377–379, Mar. 2009.

[23] S. Shin, K. Kim, and S.-M. Kang, "Compact models for memristors based on charge-flux constitutive relationships," *IEEE Trans. Comput.-Aided Design Integr. Circuits Syst.*, vol. 29, no. 4, pp. 590–598, Apr. 2010.

[24] T. Kawahara *et al.*, "2 Mb SPRAM (spin-transfer torque RAM) with Bit-by-Bit Bi-directional current write and parallelizing-direction current read," *IEEE J. Solid-State Circuits*, vol. 43, no. 1, pp. 109–120, Jan. 2008.

[25] C. Yakopcic, T. M. Taha, G. Subramanyam, R. E. Pino, and S. Rogers, "A memristor device model," *IEEE Electron Device Lett.*, vol. 32, no. 10, pp. 1436–1438, Oct. 2011.

[26] S. Kvatinsky, K. Talisveyberg, D. Fliter, E. G. Friedman, A. Kolodny, and U. C. Weiser, "Verilog-A for memristors models," in *CCIT Tech. Rep. 801*, Dec. 2011.

[27] S. Kvatinsky, E. G. Friedman, A. Kolodny, and U. C. Weiser, "Memristor-based IMPLY logic design procedure," in *Proc. IEEE Int. Conf. Comput. Design*, Oct. 2011, pp. 142–147.

[28] E. Lehtonen, J. Poikonen, M. Laiho, and W. Lu, "Time-dependency of the threshold voltage in memristive devices," in *Proc. IEEE Int. Symp. Circuits Syst.*, May 2011, pp. 2245–2248.

[29] D. Biolek, Z. Biolek, and V. Biolkova, "Pinched hysteresis loops of ideal memristors, memcapacitors, and meminductors must be 'self-crossing'," *Electron. Lett.*, vol. 47, no. 25, pp. 1385–1387, Dec. 2011.

[30] L. O. Chua, "Resistance switching memories are memristors," *Appl. Phys. A, Mater. Sci. Process.*, vol. 102, no. 4, pp. 765–783, Mar. 2011.

Shahar Kvatinsky received his B.Sc. degree in computer engineering and applied physics, and an MBA degree from the Hebrew University of Jerusalem in 2009 and 2010, respectively. He is working toward the Ph.D. degree in the Electrical Engineering Department at the Technion—Israel Institute of Technology, Haifa.

Before his Ph.D. studies he worked for Intel as a circuit designer.

Eby G. Friedman (F'00) received the B.S. degree from Lafayette College, Easton, PA, in 1979, and the M.S. and Ph.D. degrees from the University of California, Irvine, in 1981 and 1989, respectively, all in electrical engineering.

From 1979 to 1991, he was with Hughes Aircraft Company, rising to the position of Manager of the Signal Processing Design and Test Department, responsible for the design and test of high performance digital and analog ICs. He has been with the Department of Electrical and Computer Engineering at the University of Rochester, Rochester, NY, since 1991, where he is a Distinguished Professor, and the Director of the High Performance VLSI/IC Design and Analysis Laboratory. He is also a Visiting Professor at the Technion—Israel Institute of Technology. His current research and teaching interests are in high performance synchronous digital and mixed-signal microelectronic design and analysis with application to high speed portable processors and low power wireless communications. He is the author of over 400 papers and book chapters, a dozen patents, and the author or editor of 15 books in the fields of high speed and low power CMOS design techniques, 3-D design methodologies, high speed interconnect, and the theory and application of synchronous clock and power distribution networks.

Dr. Friedman is the Regional Editor of the *Journal of Circuits, Systems and Computers*, a Member of the Editorial Boards of the *Analog Integrated Circuits and Signal Processing*, *Microelectronics Journal*, *Journal of Low Power Electronics*, *Journal of Low Power Electronics and Applications*, and the IEEE *Journal on Emerging and Selected Topics in Circuits and Systems*, Chair of the IEEE Transactions on Very Large Scale Integration (VLSI) Systems steering committee, and a Member of the technical program committee of a number of conferences. He previously was the Editor-in-Chief of the IEEE Transactions on Very Large Scale Integration (VLSI) Systems, a Member of the Editorial Board of the Proceedings of the IEEE, the IEEE Transactions on Circuits and Systems—Part II: Analog and Digital Signal Processing, and *Journal of Signal Processing Systems*, a Member of the Circuits and Systems (CAS) Society Board of Governors, Program and Technical chair of several IEEE conferences, and a recipient of the University of Rochester Graduate Teaching Award and a College of Engineering Teaching Excellence Award. He is a Senior Fulbright Fellow.

Avinoam Kolodny (SM'11) received his Ph.D. degree in microelectronics from Technion—Israel Institute of Technology, Haifa, in 1980.

He joined Intel Corporation, where he was engaged in research and development in the areas of device physics, VLSI circuits, electronic design automation, and organizational development. He has been a member of the Faculty of Electrical Engineering at the Technion since 2000. His current research is focused primarily on interconnects in VLSI systems, at both physical and architectural levels.

Uri C. Weiser (F'02) received his B.S. and M.S. degrees in EE from Technion—Israel Institute of Technology, Haifa, and a Ph.D degree in CS from the University of Utah, Salt Lake City.

He is a visiting Professor at the Electrical Engineering Department, Technion IIT, and acts as an advisor at numerous startups. He worked at Intel from 1988 to 2006. At Intel, he initiated the definition of the first Pentium® processor, drove the definition of Intel's MMX™ technology, invented (with A. Peleg) the Trace Cache, co-managed and established the Intel Microprocessor Design Center at Austin, TX, and later initiated an Advanced Media applications research activity. Prior to his career at Intel, he worked for the Israeli Department of Defense as a research and system engineer and later with the National Semiconductor Design Center in Israel, where he led the design of the NS32532 microprocessor.

Dr. Weiser was appointed Intel Fellow in 1996, and in 2005 he became an ACM Fellow. He was an Associate Editor of *IEEEMicro Magazine* (1992–2004) and was Associate Editor of *Computer Architecture Letters*.